is strongly influenced by both steric *and* electronic effects, in agreement with previous findings in related systems.[2a,7]

**The Homolysis of $PhCH_2Co(dmgBF_2)_2H_2O$.** The rate constant for the decomposition of $PhCH_2Co(dmgBF_2)_2H_2O$ in the presence of $H_2O_2$, $O_2$, and HTMPO is strongly indicative of a mechanism consisting of unimolecular homolysis (eq 9), followed by faster reactions (eq 16 and 17). Additional support for this mechanism

$$Co(dmgBF_2)_2 + H_2O_2 \xrightarrow{fast} \text{products} \quad (16)$$

$$\cdot CH_2Ph + O_2 \text{ (or HTMPO)} \xrightarrow{fast} \text{products} \quad (17)$$

comes from the formation of $Co(dmgBF_2)_2$ as a product, confirmed when HTMPO is used as a scavenger. The kinetic retarding effect of the Co(II) complex confirms the equilibrium nature of the initial homolysis reaction. Moreover, the homolysis rate constants calculated from both methods agree.

The activation parameters for the rate-limiting step are also strongly supportive of a homolytic process. The high enthalpy of activation (28.6 kcal/mol) is expected for an unassisted homolytic bond-breaking process. High positive entropies of activation have been observed before in the homolytic metal–carbon bond cleavage reactions in aqueous solvents,[2,4,6] in keeping with that $\Delta S^{\ddagger} = 14.0$ cal $mol^{-1}$ $K^{-1}$ in this reaction. It is interesting to note that $\Delta S^{\ddagger}$ values in nonaqueous solvents are much lower, typically close to 0,[48] suggesting at least two contributions to the $\Delta S^{\ddagger}$ term: the intrinsic contribution due to the radical dissociation and the effect of the release of the purely organic species on the structure of surrounding water. The latter effect appears to be quite substantial. The same conclusion has been reached independently by the group which has determined $\Delta V^{\ddagger}$ for the homolysis of $(H_2O)_5CrR^{2+}$ complexes.[49]

The rate constants are now known for the homolysis of $PhCH_2Co(dmgBF_2)_2$ ($k = 7.58 \times 10^{-6}$ $s^{-1}$ at 25 °C) and $PhCH_2Cr^{2+}$ ($k = 2.63 \times 10^{-3}$ $s^{-1}$).[1] Combined with the equilibrium constant for the benzyl group transfer, $K = 2.80 \times 10^{-3}$, we calculate the ratio of the rate constants $k_{-H(Co)}/k_{-H(Cr)} = 1.03$. The measured value of $k_{-H(Cr)}$ is $8.5 \times 10^7$ $M^{-1}$ $s^{-1}$,[50] and thus $k_{-H(Co)} = 8.8 \times 10^7$ $M^{-1}$ $s^{-1}$.[51] Both rate constants fall in the general range expected[24-26] for the recombination of metal complexes with carbon-centered radicals.

The calculated free energy of activation for the reactions of $Co(dmgBF_2)_2$ with $\cdot CH_2Ph$ at 25 °C is $\Delta G^{\ddagger} = 6.5$ kcal/mol. The high $\Delta S^{\ddagger}_{H(Co)}$ in the forward direction of reaction 9 implies $\Delta S^{\ddagger}_{-H(Co)} \lesssim 0$ for the reverse reaction. Taking $\Delta S^{\ddagger}_{-H(Co)} \simeq 0$ to −10 cal/(mol K), $\Delta H^{\ddagger}_{-H(Co)}$ for the reaction of $Co(dmgBF_2)_2$ with $\cdot CH_2Ph$ has a value of $\sim 5 \pm 2$ kcal/mol. The difference between the activation enthalpies for the forward and reverse reaction, $\Delta H^{\ddagger}_{H(Co)} - \Delta H^{\ddagger}_{-H(Co)}$, gives directly the Co–C bond energy, BDE = 24 ± 3 kcal/mol. This value is close to the previously published BDE's for similar organocobalt complexes.[3]

**Acknowledgment.** This work was supported by the U.S. Department of Energy, Office of Basic Energy Sciences, Chemical Sciences Division, under Contract W-7405-ENG-82. A.B. acknowledges the NATO support, Grant No. 559/83, and useful discussions with Dr. A. Petrou.

(48) The only exception seems to be $RCo[C_2(DO)(DOH)_{pn}]I$[13] with $\Delta S^{\ddagger}$ = 8 cal $mol^{-1}$ $K^{-1}$ (R = $PhCH_2$) and 18 cal $mol^{-1}$ $K^{-1}$ (R = $(CH_3)_3CCH_2$) in *o*-dichlorobenzene.

(49) Rindermann, W.; van Eldik, R.; Sisley, M. J.; Swaddle, T. W., unpublished observations (private communication).

(50) Blau, R. J.; Espenson, J. H.; Bakac, A. *Inorg. Chem.*, in press.

(51) $k_S$ for the reaction of $Co(dmgBF_2)_2$ with HTMPO falls in the same range, $k = 7.5 \times 10^7$ $M^{-1}$ $s^{-1}$, since $k_{-H}/k_S \simeq 1.18$.

# Coordinative Interactions in Chelated Complexes of Silicon. 13.[1] Experimental Determination of the Electron Deformation Density of a Pentacoordinated Silicon Complex†

**G. Klebe, J. W. Bats, and H. Fuess***

*Contribution from the Institut für Kristallographie und Mineralogie der Universität Frankfurt/Main, 6000 Frankfurt/Main 1, West Germany.* *Received September 19, 1983*

**Abstract:** The electron deformation density in the pentacoordinated trigonal-bipyramidal 1-(trichlorosilyl)-1,2,3,4-tetrahydro-1,10-phenanthroline ($(C_{12}H_{11}N_2)SiCl_3$, monoclinic, $P2_1/m$, $a = 9.243$ (4) Å, $b = 7.076$ (2) Å, $c = 10.739$ (4) Å, $\beta = 114.97$ (3)°, $Z = 2$) was determined by combined X-ray and neutron diffraction. Neutron data (3356 measurements) were collected at $\lambda = 0.894$ Å (up to $(\sin\theta)/\lambda = 0.89$ $Å^{-1}$, 1617 unique observations) and 1.266 Å ($(\sin\theta)/\lambda_{max} = 0.63$ $Å^{-1}$, 1428 unique data) at 120 K; X-ray intensities were measured with Mo Kα radiation at 120 K up to $(\sin\theta)/\lambda = 0.81$ $Å^{-1}$ (11 997 measurements, 3008 unique). The molecule contains two different Si–N bonds. The shorter one (1.746 (2) Å), located in the equatorial plane, is introduced by chemical substitution reaction. The X–N maps reveal a maximum of 0.4 e/$Å^3$ between Si and N in this equatorial bond, and maxima of the lone pair density, expected below and above the position of the trivalent nitrogen, are significantly displaced toward Si. This release of density into the Si–N bond might explain the "contraction" of the Si–N bond as compared with the sum of the covalent radii (1.87 Å). The axial Si–N bond (1.979 (2) Å) results from an intramolecular coordinative interaction. The lone pair of the coordinated "pyridine" nitrogen (centered 0.7 Å from N) is strongly polarized by silicon and the two equatorial chlorine atoms. The density distribution in the two topologically different Si–Cl bonds is rather low and diffuse.

In contrast to carbon, silicon is able to expand its valence shell from tetravalency to penta- and hexacoordination, forming well-defined stable compounds. These extracoordinated silicon derivatives can either be cations or anions or uncharged coordination complexes in which the valence shell expansion is achieved by Lewis acid–base interaction. For these coordinative interactions, interatomic distances in the range between "normal single" bonds and pure van der Waals contacts are observed.

† Presented at the 7th European Crystallographic Meeting in Jerusalem (1982) and the AGKr-Tagung in Tübingen (1983).

(1) Part 12: Klebe, G.; *J. Chem. Soc., Dalton Trans.*, submitted for publication.

0002-7863/84/1506-5202$01.50/0 

**Scheme I**

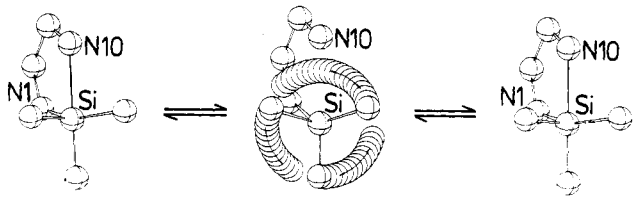


The crystal structure determination[2] of 1-(trichlorosilyl)-1,2,3,4-tetrahydro-1,10-phenanthroline (**1**), an example belonging

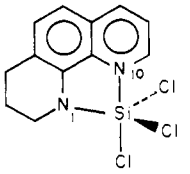


**1**

to the latter group, revealed a pentacoordinate trigonal-bipyramidal geometry around silicon. The central atom is bonded in the equatorial plane to the amino-type nitrogen N1 in the higher saturated ring through a Si–N "single" bond (1.746 (2) Å). It is introduced by chemical substitution reaction of the lithiated ligand with $SiCl_4$. A coordinative Si···N10 bond (1.979 (2) Å), axial with respect to silicon, is formed by intramolecular Lewis acid–base interaction between silicon and the tertiary pyridine-type nitrogen N10 in the lower hydrogenated ring.

The two Si–N connections show pronounced differences in length and stability. Crystal structure analysis of closely related silicon complexes with the same ligand revealed that the elongation of the coordinative bond (Si–N10) amounts to 13–54% with respect to the Si–N1 "single" bond in dependence on the substitution on silicon ($-SiF_3$, $-SiCl_3$, $-SiMeCl_2$, $-SiMe_2Cl$, $-SiMe_3$).[1-4] Extensive NMR investigations in solution[5-8] of these complexes and closely related derivatives demonstrated that the coordinative bond is labile, and dynamic NMR studies revealed intramolecular exchange of substituents at silicon. This positional exchange of substituents at pentacoordinate silicon is explained by a bond rupture/bond re-formation mechanism involving a rotation of an intermediate tetracoordinate silyl group (Scheme I). The exchange barrier amounts to 7–18 kcal/mol. It is composed of the activation energy of the rotational freedom and of the contribution to overcome the coordinative Si···N interaction. This energy barrier is small and comparable with those observed for bulky side groups such as *tert*-butyl at aromatic ring systems.

It is therefore of interest to determine whether the coordinative donor–acceptor interaction leads to a noticeable polarization of the "lone" pair at the pyridine-type nitrogen N10. The trigonal-bipyramidal arrangement can result as the most favorable configuration when the rotational movement of the silyl group detected in solution is frozen in the solid state. The $SiR_3$ group "clicks" into the observed position because of an electrostatic attraction between the ligand N10 atom and the central Si atom, which are presumably slightly different in charge.

The shorter Si–N1 bond displays a length of 1.746 (2) Å, which is near the arithmetic mean value of 1.75 Å, observed for bonds between silicon and trivalent nitrogen in tetra- and pentacoordinated compounds (extremes: 1.69–1.81 Å, omitting structures of silyl amides). Pauling[9] and Shomaker and Stevenson[10] calculated covalent radii for Si and N. The sum of these values amounts to 1.87 Å (Pauling) or 1.80 Å (Shomaker and Stevenson), both longer than our experimental bond length. This "contraction" the Si–N bond has often been discussed in terms of "partial doubling bonding character". It is of interest to know whether this "contraction" leads to any noticeable mutual polarization of the experimentally determined electron density between Si and N.

In order to investigate the electronic nature of the two different Si–N bonds in the present class of chelated silicon complexes, an electron density study of **1**, employing the X–N method, was performed.

**Table I.** Experimental Conditions during Data Collection and Lattice Constants

$a$ = 9.243 (4) Å, $b$ = 7.076 (2) Å, $c$ = 10.739 (4) Å, $\beta$ = 114.97 (3)°, $V$ = 636.7 (5) Å$^3$, $z$ = 2, space group $P2_1/m$

| | neutrons | neutrons | X-rays |
|---|---|---|---|
| wavelength, Å | 1.266 | 0.894 | 0.71069 |
| $(\sin\theta)/\lambda_{max}$, Å$^{-1}$ | 0.627 | 0.888 | 0.809 |
| $\mu$, cm$^{-1}$ | | 1.51 | 7.20 |
| transmission | 0.78–0.88 | 0.79–0.89 | 0.83–0.94 |
| measured refl. | 1677 | 1679 | 11997 |
| unique refl.[a] | 1428 | 1617 | 3008 |
| $R(I)$ | 0.029 | 0.030 | 0.042 |
| $R(F)$ | 0.028 | 0.030 | 0.055 |
| $R_w(F)$ | 0.035 | 0.028 | 0.031 |

[a] After averaging.

## Experimental Section

The title compound $(C_{12}H_{11}N_2)SiCl_3$, was prepared as described by Hensen and Klebe.[11] Single crystals were obtained from repeated sublimation under vacuum through a temperature gradient of 140/143 °C. The growth of suitable crystals for neutron diffraction took about 3 weeks. The cell constants at 120 K were determined and refined from the angular settings of 15 reflections in the X-ray diffraction experiment. Due to their pronounced sensitivity to moisture, the crystals had to be encapsulated. The specimens for X-ray diffraction were sealed under dried argon into thin glass capillaries. The samples for neutron diffraction were mounted on aluminum pins, and crystal and pin were enclosed in an airtight capsule made of quartz glass (diameter, 6 mm; wall thickness, 0.03 mm).

**Neutron Diffraction.** The data collection was performed on a parallelopiped crystal with the dimensions 1.09 × 1.00 × 4.62 mm$^3$. The quality of the crystal was checked by neutron Laue photographs. The intensities were measured on the computer-controlled diffractometer D8 at ILL, Grenoble. The crystal mount was enclosed in an Air Products Displex Cryostat,[12] and the experiment was performed at 120 K. A thermocouple recording the temperature had been calibrated by using the phase transition of $KH_2PO_4$ at 122.8 K. Data were measured at two different wavelengths of 1.266 (2) and 0.894 (2) Å (calibrated by a single crystal of NaCl). Other conditions during the measurments are reported in Table I. Three control reflections ($\bar{5}01$, 611, 04$\bar{8}$) remeasured after every 60 reflections did not display significant fluctuations. Data were corrected for absorption. The absorption coefficient was determined experimentally from two different crystals. Background correction was made by profile analysis.[13] A weight $w(I) = 1/[\sigma^2(I)_{count} + (0.03I)^2]$ was assigned to each reflection. Symmetry equivalent observations were averaged.

**X-ray Diffraction.** The X-ray diffraction experiment was carried out on a Syntex $P2_1$ diffractometer using Nb-filtered Mo K$\alpha$ radiation. A temperature of 120 K was maintained during the experiment by use of an Enraf-Nonius low-temperature device. A thermocouple mounted in the cold gas stream was calibrated by the phase transition of $KH_2PO_4$. The actual temperature fluctuations are estimated to ±3 °C during data collection. The crystal used had a size of 0.094 × 0.245 × 0.453 mm$^3$. Background corrections were applied by profile analysis following the formalism described by Blessing, Coppens, and Becker.[14] Three standard reflections (4$\bar{1}\bar{2}$, 1$\bar{2}\bar{2}$, 22$\bar{1}$) monitored after 60 observations showed

(2) Part 3: Klebe, G.; Bats, J. W.; Hensen, K. *Z. Naturforsch., B* **1983**, *38B*, 825.
(3) Part 4: Klebe, G.; Hensen, K.; Fuess, H. *Chem. Ber.* **1983**, *116*, 3125.
(4) Part 5: Klebe, G.; Bats, J. W.; Hensen, K. *J. Chem. Soc., Dalton Trans.*, in press.
(5) Part 6: Klebe, G.; Hensen, K.; Jouanne, J. V. *J. Organomet. Chem.* **1983**, *258*, 137.
(6) Part 7: Klebe, G.; Hensen, K. *J. Chem. Soc., Dalton Trans.*, in press.
(7) Part 8: Corriu, R. J. P.; Hensen, K.; Klebe, G.; Nix, M.; Poirier, M.; Royo, G. in preparation.
(8) Part 9: Klebe, G.; Nix, M.; Hensen, K. *Chem. Ber.* **1984**, *117*, 797.
(9) Pauling, L. "The Nature of the Chemical Bond"; Cornell University Press: Ithaca, NY, 1960.
(10) Shomaker, V.; Stevenson, D. P. *J. Am. Chem. Soc.* **1941**, *63*, 1941.
(11) Part 1: Hensen, K.; Klebe, G. *J. Organomet. Chem.* **1981**, *207*, 19.
(12) Allibon, J. R.; Filhol, A.; Lehmann, M. S.; Mason, S. A.; Simms, P. *J. Appl. Cryst.* **1981**, *14*, 326.
(13) Lehmann, M. S.; Larson, F. K. *Acta Crystallogr., Sect. A* **1974**, *A30*, 580.
(14) Blessing, R. H.; Coppens, P.; Becker, P. *J. Appl. Crystallogr.* **1974**, *7*, 488.

maximal long-range fluctuation of 6%, which is attributed to variations in incident beam intensity and counter response. The data were scaled with respect to the three standard reflections. Absorption correction was made by numerical integration. The equivalent observations were averaged and weights were assigned as described in the neutron diffraction case.

**Structure Refinements. Neutron Data.** Scattering lengths were taken from Koester.[15] The two data sets obtained at different wavelengths were treated separately. Averaging of the two sets did not improve the agreement factors in refinement. The structural parameters of the room-temperature X-ray structure determination reported by Klebe, Bats, and Hensen[2] were used as starting values. As already discussed,[2] the refinement was based on the centric space group $P2_1/m$, implying that Si, Cl1, N1, N10, all carbons except C3, and the hydrogen bound to the benzoic rings occupy a special position on $m$. The carbon C3 and the H atoms bound to C2, C3, and C4 are statistically disordered in half-occupancy ($pp = 0.5$) above and below the mirror plane. Cl2 a general position ($pp = 1$) and the second chlorine atom in the equatorial plane is generated by mirro symmetry. The refinements of extinction coefficients were made using the LINEX program of Becker and Coppens.[16] Refinements were based on $F^2$. Data measured at wavelength 1.266 Å were more affected by extinction than those measured at 0.894 Å. Refinement of isotropic extinction with the data at 0.894 Å revealed a less than 1% extinction effect. For all X–N studies reported in this paper, the parameters derived from neutron data at 0.894 Å were used. The positional parameters and the anisotropic temperature factors from the neutron data at 0.894 Å are reported in Tables II and III. The final agreement factors are given in Table I.

**X-ray Data.** Scattering factors were from Fukamachi.[17] All refinements were based on $F$. Anomalous dispersion factors[18] were applied to Si and Cl. The isotropic extinction coefficient was refined by use of the LINEX program.[16] The results show that the influence of extinction can be neglected. In all calculations the positional and thermal parameters of hydrogen were taken as determined by neutron diffraction. Refinements were performed by using all the X-ray data and just the data with $(\sin\theta)/\lambda > 0.70$ Å$^{-1}$. The results of the all-data refinement are listed in Tables II and III. For the high-angle refinement the extinction coefficient was kept invariant, and the scale factor was refined separately. It varies in dependence on the $(\sin\theta)/\lambda$ cut-off in reciprocal space. The final agreement factors are listed in Table I.

**Difference Density.** The positional parameters derived from refinement of the neutron data, X-ray all data and X-ray high-order data are very similar (Table II). The average deviation is $(1-2)\sigma$; the maximum corresponds to $5\sigma$ in the $z$-coordinate of Cl1.

The agreement is not as good when the thermal parameters are considered (Table III). The values refined from neutron data are generally smaller than those obtained from X-rays. This may indicate a possible difference in temperature during the two experiments. But temperature as the sole reason for this effect cannot explain that the discrepancy between temperature factors varies with direction. The differences are nearly twice as large in $U_{11}$ as in $U_{22}$ and $U_{33}$. For the diagonal term $U_{13}$ the smallest deviation is found. Similar trends are often found in combined X-ray and neutron investigations.[19] A possible explanation for this effect is diffuse scattering which contributes to the reflections. The systematic deviations in thermal parameters have to be taken into account when the deformation density is calculated from data obtained from neutron and X-ray diffraction (X–N method).

Throughout this paper difference density maps have been calculated by using the X-ray data up to $(\sin\theta)/\lambda = 0.81$ Å$^{-1}$. In all syntheses the positional parameters are from the neutron data. Unique thermal parameters were obtained by a combination of X-ray and neutron temperature factors. To each $U_{ij}$ (N) the difference $[U_{ij}(\text{x·high order}) - U_{ij}(\text{N})]$, which was weighted $(1/\sigma^2)$ and averaged over all atoms, was added.

The difference density maps (X–N method) were calculated with the SPFT program[20] using all reflections of X-ray data with the scale factor from high-angle refinement. When the difference Fourier coefficients were calculated, the effect of anomalous dispersion was taken into account.[21] A comparison with the density maps solely derived from X-ray data (X–X method) shows that the information between the atoms is rather similar. Differences can be detected in the vicinity of the atoms.

Maps calculated with different scale factors show pronounced variation in the "depth of the density holes" on Si and Cl and the density distribution in the nearer surroundings of Cl. Off the atomic centers density distribution remains nearly unaffected and can be used for qualitative interpretations of mutual polarization of the bonding electrons by the atoms in the molecule. By use of the program system of Matthewman et al.[22] error maps were calculated, which show that the accuracy of the density maps might be estimated to 0.15–0.2 e/Å$^3$ within $3\sigma$.

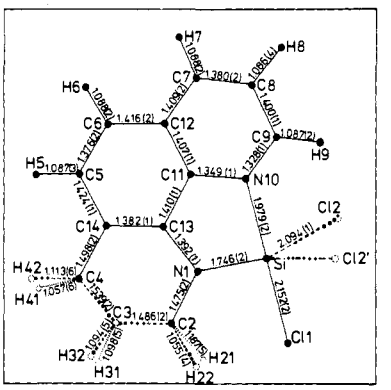


**Figure 1.** Bond lengths [Å] based on neutron data (esd in parentheses).

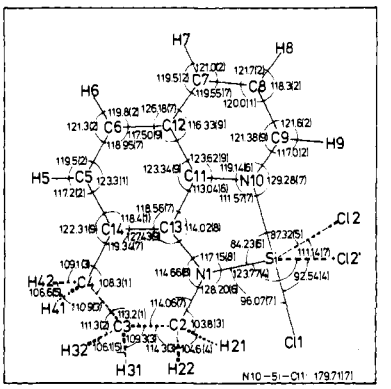


**Figure 2.** Interatomic angles [deg] based on neutron data (esd in parentheses).

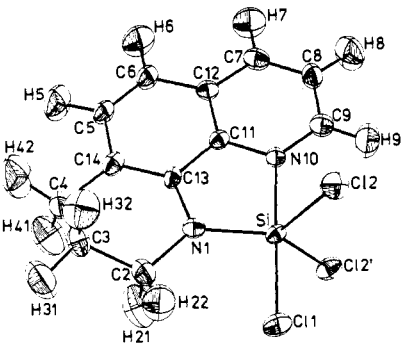


**Figure 3.** ORTEP drawing of **1**; the thermal ellipsoids are the 95% probability surfaces.

## Discussion

Bond distances and angles, based on neutron data, are given in Figures 1 and 2. An ORTEP plot of **1** is shown in Figure 3. The trigonal-bipyramidal structure of the present Si-chelated complex has been described in detail in the X-ray crystal structure determination at room temperature.[2]

The difference density in the "molecular plane" (coincident with the crystallographic mirror plane $m$ in $P2_1/m$, $y = 0.25$, with the

(15) Koester, L. "Neutron Physics", Springer Tracts in Modern Physics; Höhler, G., Ed.; Springer-Verlag: Berlin, 1977, Vol. 80.
(16) Becker, P. J.; Coppens, P. *Acta Crystallogr., Sect. A* **1975**, *A31*, 417.
(17) Fukamachi, T. *Solid State Phys. (Tokyo), Ser. B* **1971**, *No. 12*.
(18) Cromer, D. T.; Waber, J. T. "International Tables for X-ray Crystallography"; Kynoch Press: Birmingham, England, 1974, Vol. IV.
(19) Coppens, P.; Boehme, R.; Price, P. F.; Stevens, E. D. *Acta Crystallogr., Sect. A* **1981**, *A37*, 857. Fuess, H.; Bats, J. W.; Dannöhl, H.; Meyer, H.; Schweig, A. *Acta Crystallogr., Sect. B* **1982**, *B38*, 736. Elerman, Y.; Bats, J. W.; Fuess, H. *Acta Crystallogr., Sect. C* **1983**, *C39*, 515.
(20) v. de Waal, B. W. "Slant Plane Fourier Transform Program", Dept. of Physics, University of Twente, Enschede, Netherlands, 1975.
(21) Yang, Y. W., Coppens, P. *Solid State Commun.* **1974**, *15*, 1555.
(22) Matthewman, J. C.; Thompson, P.; Brown, P. J. *J. Appl. Crystallogr.* **1982**, *15*, 167.

**Table II.** Positional Parameters from Neutron (N, 0.894 Å) and X-ray (X) Data[a]

| atom | | x | y | z |
|---|---|---|---|---|
| Cl1 | N | 0.39648 (7) | 0.25000 (0) | 0.01264 (6) |
| Cl1 | X | 0.39647 (5) | 0.25000 (0) | 0.01292 (4) |
| Cl2 | N | 0.46712 (5) | 0.49407 (7) | 0.26788 (5) |
| Cl2 | X | 0.46722 (4) | 0.49388 (5) | 0.26803 (3) |
| Si | N | 0.5658 (13) | 0.25000 (0) | 0.2248 (12) |
| Si | X | 0.56573 (6) | 0.25000 (0) | 0.22485 (5) |
| N1 | N | 0.73611 (6) | 0.25000 (0) | 0.19304 (6) |
| N1 | X | 0.7358 (2) | 0.25000 (0) | 0.1935 (1) |
| N10 | N | 0.72060 (6) | 0.25000 (0) | 0.42026 (6) |
| N10 | X | 0.7204 (2) | 0.25000 (0) | 0.4201 (1) |
| C13 | N | 0.88320 (9) | 0.25000 (0) | 0.30667 (8) |
| C13 | X | 0.8831 (2) | 0.25000 (0) | 0.3069 (2) |
| C11 | N | 0.87246 (9) | 0.25000 (0) | 0.43376 (8) |
| C11 | X | 0.8724 (2) | 0.25000 (0) | 0.4337 (2) |
| C2 | N | 0.7454 (12) | 0.25000 (0) | 0.0592 (10) |
| C2 | X | 0.7454 (2) | 0.25000 (0) | 0.0587 (2) |
| C3[b] | N | 0.8934 (2) | 0.3367 (2) | 0.0626 (1) |
| C3[b] | X | 0.8934 (3) | 0.3376 (4) | 0.0628 (2) |
| C4 | N | 1.0466 (1) | 0.25000 (0) | 0.1728 (1) |
| C4 | X | 1.0462 (2) | 0.25000 (0) | 0.1722 (2) |
| C5 | N | 1.1689 (1) | 0.25000 (0) | 0.4356 (1) |
| C5 | X | 1.1690 (2) | 0.25000 (0) | 0.4357 (2) |
| C6 | N | 1.1590 (1) | 0.25000 (0) | 0.5600 (1) |
| C6 | X | 1.1593 (2) | 0.25000 (0) | 0.5602 (2) |
| C7 | N | 0.9754 (1) | 0.25000 (0) | 0.67894 (9) |
| C7 | X | 0.9750 (2) | 0.25000 (0) | 0.6786 (2) |
| C8 | N | 0.8196 (1) | 0.25000 (0) | 0.66389 (9) |
| C8 | X | 0.8200 (2) | 0.25000 (0) | 0.6638 (2) |
| C9 | N | 0.6937 (1) | 0.25000 (0) | 0.53235 (9) |
| C9 | X | 0.6943 (2) | 0.25000 (0) | 0.5329 (2) |
| C12 | N | 1.00656 (9) | 0.25000 (0) | 0.56133 (8) |
| C12 | X | 1.0064 (2) | 0.25000 (0) | 0.5615 (2) |
| C14 | N | 1.03275 (9) | 0.25000 (0) | 0.30685 (9) |
| C14 | X | 1.0323 (2) | 0.25000 (0) | 0.3071 (2) |
| H9 | N | 0.5698 (3) | 0.25000 (0) | 0.5174 (3) |
| H8 | N | 0.7909 (4) | 0.25000 (0) | 0.7521 (3) |
| H7 | N | 1.0747 (3) | 0.25000 (0) | 0.7804 (2) |
| H6 | N | 1.2658 (3) | 0.25000 (0) | 0.6565 (3) |
| H5 | N | 1.2854 (3) | 0.25000 (0) | 0.4335 (3) |
| H21[b] | N | 0.7476 (6) | 0.0870 (6) | 0.0337 (5) |
| H22[b] | N | 0.6393 (4) | 0.3018 (8) | −0.0197 (3) |
| H31[b] | N | 0.8932 (5) | 0.3251 (9) | −0.3945 (4) |
| H32[b] | N | 0.8854 (5) | 0.4877 (6) | 0.0806 (5) |
| H41[b] | N | 1.0668 (7) | 0.1134 (8) | 0.1435 (5) |
| H42[b] | N | 1.1509 (6) | 0.338 (1) | 0.1830 (5) |

[a] Estimated standard deviations in parentheses. N: Refinement based on neutron data at 0.894 Å. X: X-ray all-data refinement. [b] Half populated.

atoms N1, C2, C4, C13, C14, C5, C6, C11, C12, C7, C8, C9, N10, Si, Cl1, H5, H6, H7, H8, H9; see Table II) is shown in Figure 4. The density maxima (0.4–0.8 e/Å$^3$) between the carbon atoms of the aromatic ring system are in the same range as in many other studies. They can be used as "standard" for the comparison of different experiments (cf. problem of the scale factor).

**Density in the Donor–Acceptor Si–N10 Bond.** The coordinative Si–N10 bond is 13.3% extended compared with the Si–N1 "single bond". The lone pair on the pyridine-type nitrogen is strongly polarized by the neighboring silicon. The center of the electron density between these two atoms is about 0.7 Å apart from N10. The density distribution is strongly deformed in direction to silicon and shows a slower decrease along the Si–N10 axis in direction to silicon than to N10. In contrast, the increase of charge density in the Si–N1 "single bond" is much steeper starting from silicon than from N1 and the center of charge is about 1 Å apart from N1. Furthermore, the density in the coordinative bond is polarized by the two equatorial chlorine atoms. This distortion is indicated in Figures 4 and 5. It is shown as well in the left-hand part of Figure 6 in two parallel sections perpendicular to the bond axis Si–N10 and the molecular plane.

A section through the coordinative bond perpendicular to the molecular plane and parallel to the Si–N10 bond axis (Figure 7)

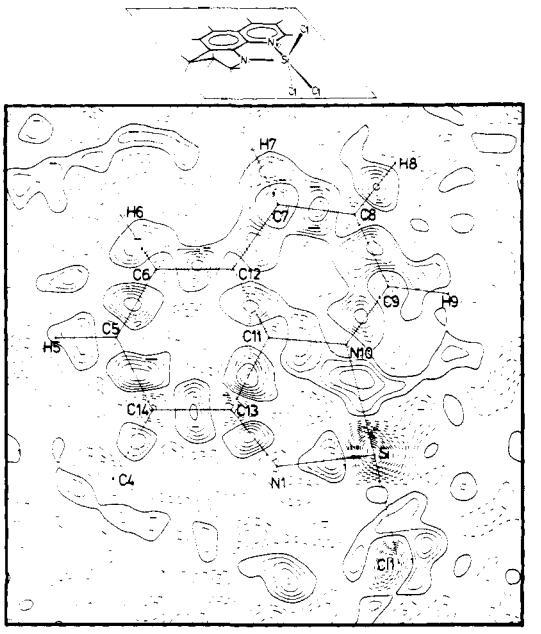


**Figure 4.** Deformation density in the crystallographic mirror plane *m* (herein after "molecular plane") of $P2_1/m$ ($y$ = 0.25) containing the major part of the molecule (all atoms with $y$ = 0.25, see Table II); contour level 0.1 e/Å$^3$, zero line ommited, negative contours broken.

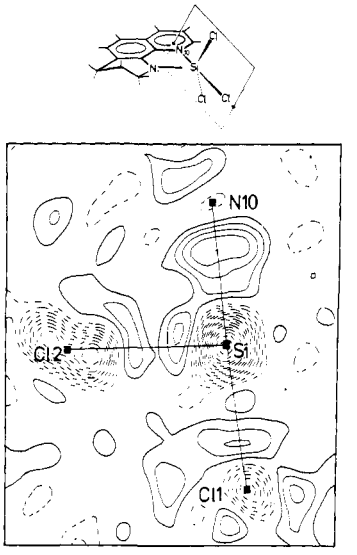


**Figure 5.** Deformation density in the plane through N10, Si, Cl1, and Cl2 (contours as in Figure 3).

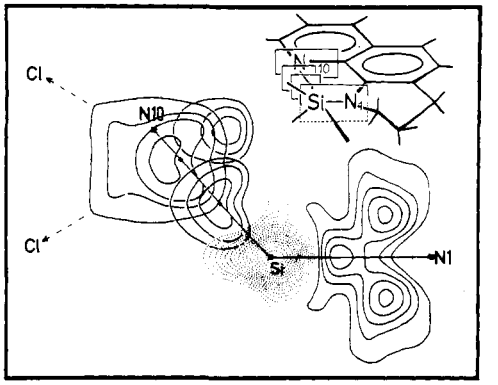


**Figure 6.** Deformation density in the two different Si–N bonds. Left: parallel sections perpendicular to the Si–N10 bond. Right: section through the Si–N1 bond (contours as in Figure 3).

demonstrates on the left-hand side the electron withdrawal from the lone-pair region at N10 in direction to Si. The density dis-

**Table III.** Thermal Parameters Multiplied by 100 Derived from Neutron Diffraction (N, 0.894 Å), X-ray All Data (X) and High-Order Data (XH, 0.7–0.81 Å$^{-1}$)[a]

| atom | | $U_{11}$ | $U_{22}$ | $U_{33}$ | $U_{12}$ | $U_{13}$ | $U_{23}$ |
|---|---|---|---|---|---|---|---|
| Cl1 | N | 1.28 (2) | 2.65 (3) | 1.28 (2) | 0.000 (0) | 0.03 (2) | 0.000 (0) |
| Cl1 | X | 1.37 (2) | 2.63 (2) | 1.38 (2) | 0.000 (0) | 0.04 (2) | 0.000 (0) |
| Cl1 | XH | 1.41 (4) | 2.62 (5) | 1.45 (4) | 0.000 (0) | 0.08 (3) | 0.000 (0) |
| Cl2 | N | 1.47 (1) | 1.54 (2) | 1.90 (2) | 0.44 (1) | 0.54 (1) | −0.06 (1) |
| Cl2 | X | 1.66 (1) | 1.57 (1) | 2.01 (1) | 0.47 (1) | 0.58 (1) | −0.08 (1) |
| Cl2 | XH | 1.75 (2) | 1.62 (2) | 1.97 (2) | 0.48 (2) | 0.59 (2) | −0.06 (2) |
| Si | N | 0.72 (3) | 1.04 (4) | 1.10 (4) | 0.000 (0) | 0.29 (3) | 0.000 (0) |
| Si | X | 0.96 (2) | 1.27 (2) | 1.24 (2) | 0.000 (0) | 0.32 (2) | 0.000 (0) |
| Si | XH | 0.89 (4) | 1.23 (4) | 1.21 (4) | 0.000 (0) | 0.28 (3) | 0.000 (0) |
| N1 | N | 0.93 (2) | 1.47 (2) | 0.99 (2) | 0.000 (0) | 0.37 (1) | 0.000 (0) |
| N1 | X | 1.05 (6) | 1.84 (7) | 1.03 (6) | 0.000 (0) | 0.31 (5) | 0.000 (0) |
| N1 | XH | 1.3 (1) | 1.4 (1) | 1.1 (1) | 0.000 (0) | 0.3 (1) | 0.000 (0) |
| N10 | N | 0.82 (2) | 1.47 (2) | 0.97 (2) | 0.000 (0) | 0.34 (1) | 0.000 (0) |
| N10 | X | 1.03 (6) | 1.44 (7) | 1.30 (6) | 0.000 (0) | 0.43 (5) | 0.000 (0) |
| N10 | XH | 1.1 (1) | 1.6 (1) | 1.0 (1) | 0.000 (0) | 0.40 (9) | 0.000 (0) |
| C13 | N | 0.80 (2) | 0.99 (3) | 1.08 (3) | 0.000 (0) | 0.41 (2) | 0.000 (0) |
| C13 | X | 1.08 (7) | 1.10 (7) | 1.45 (7) | 0.000 (0) | 0.46 (6) | 0.000 (0) |
| C13 | XH | 0.9 (1) | 1.5 (1) | 1.4 (1) | 0.000 (0) | 0.6 (1) | 0.000 (0) |
| C11 | N | 0.70 (2) | 1.11 (3) | 0.93 (3) | 0.000 (0) | 0.25 (2) | 0.000 (0) |
| C11 | X | 1.08 (7) | 1.08 (7) | 1.33 (7) | 0.000 (0) | 0.37 (6) | 0.000 (0) |
| C11 | XH | 1.0 (1) | 1.2 (1) | 1.2 (1) | 0.000 (0) | 0.4 (1) | 0.000 (0) |
| C2 | N | 1.46 (3) | 2.77 (5) | 1.13 (3) | 0.000 (0) | 0.61 (3) | 0.000 (0) |
| C2 | X | 1.83 (9) | 3.1 (1) | 1.30 (7) | 0.000 (0) | 0.81 (7) | 0.000 (0) |
| C2 | XH | 2.0 (2) | 2.5 (2) | 1.5 (2) | 0.000 (0) | 0.9 (1) | 0.000 (0) |
| C3 | N | 1.69 (4) | 1.98 (6) | 1.39 (4) | −0.21 (4) | 0.91 (4) | 0.07 (4) |
| C3 | X | 1.9 (1) | 2.3 (1) | 1.56 (10) | −0.2 (1) | 1.01 (9) | 0.05 (10) |
| C3 | XH | 2.3 (2) | 1.9 (3) | 1.7 (2) | 0.0 (2) | 1.2 (2) | 0.5 (2) |
| C4 | N | 1.44 (3) | 2.29 (4) | 1.88 (4) | 0.000 (0) | 1.06 (3) | 0.000 (0) |
| C4 | X | 1.63 (9) | 2.9 (1) | 2.09 (8) | 0.000 (0) | 1.13 (7) | 0.000 (0) |
| C4 | XH | 1.7 (2) | 2.8 (2) | 1.9 (2) | 0.000 (0) | 1.0 (1) | 0.000 (0) |
| C5 | N | 0.77 (3) | 2.19 (4) | 1.82 (3) | 0.000 (0) | 0.43 (2) | 0.000 (0) |
| C5 | X | 1.07 (7) | 2.07 (9) | 2.39 (9) | 0.000 (0) | 0.65 (7) | 0.000 (0) |
| C5 | XH | 0.8 (1) | 2.5 (2) | 1.7 (2) | 0.000 (0) | 0.3 (1) | 0.000 (0) |
| C6 | N | 0.81 (3) | 2.04 (4) | 1.57 (3) | 0.000 (0) | 0.15 (3) | 0.000 (0) |
| C6 | X | 1.09 (7) | 2.14 (9) | 1.82 (8) | 0.000 (0) | 0.20 (6) | 0.000 (0) |
| C6 | XH | 1.0 (1) | 2.5 (2) | 1.7 (2) | 0.000 (0) | 0.4 (1) | 0.000 (0) |
| C7 | N | 1.36 (3) | 1.82 (4) | 1.02 (3) | 0.000 (0) | 0.23 (2) | 0.000 (0) |
| C7 | X | 1.94 (9) | 1.76 (9) | 1.35 (8) | 0.000 (0) | 0.31 (7) | 0.000 (0) |
| C7 | XH | 2.1 (2) | 2.1 (2) | 1.2 (1) | 0.000 (0) | 0.5 (1) | 0.000 (0) |
| C8 | N | 1.54 (3) | 2.19 (4) | 1.07 (3) | 0.000 (0) | 0.53 (2) | 0.000 (0) |
| C8 | X | 2.20 (9) | 2.02 (9) | 1.47 (8) | 0.000 (0) | 0.82 (7) | 0.000 (0) |
| C8 | XH | 1.7 (2) | 2.6 (2) | 1.6 (2) | 0.000 (0) | 0.9 (1) | 0.000 (0) |
| C9 | N | 1.19 (3) | 2.22 (4) | 1.10 (3) | 0.000 (0) | 0.56 (2) | 0.000 (0) |
| C9 | X | 1.70 (8) | 2.05 (9) | 1.55 (8) | 0.000 (0) | 0.77 (7) | 0.000 (0) |
| C9 | XH | 1.7 (2) | 2.1 (2) | 1.4 (2) | 0.000 (0) | 0.5 (1) | 0.000 (0) |
| C12 | N | 0.87 (2) | 1.32 (3) | 1.08 (3) | 0.000 (0) | 0.12 (2) | 0.000 (0) |
| C12 | X | 1.22 (7) | 1.30 (8) | 1.29 (7) | 0.000 (0) | 0.18 (6) | 0.000 (0) |
| C12 | XH | 1.2 (1) | 1.5 (1) | 1.2 (1) | 0.000 (0) | 0.3 (1) | 0.000 (0) |
| C14 | N | 0.89 (3) | 1.41 (3) | 1.47 (3) | 0.000 (0) | 0.58 (2) | 0.000 (0) |
| C14 | X | 1.35 (8) | 1.45 (8) | 1.81 (8) | 0.000 (0) | 0.75 (7) | 0.000 (0) |
| C14 | XH | 1.1 (1) | 1.5 (1) | 2.0 (2) | 0.000 (0) | 0.6 (1) | 0.000 (0) |
| H9 | N | 1.99 (8) | 5.78 (16) | 2.60 (8) | 0.000 (0) | 1.21 (7) | 0.000 (0) |
| H8 | N | 3.51 (11) | 6.03 (18) | 1.99 (8) | 0.000 (0) | 1.48 (8) | 0.000 (0) |
| H7 | N | 2.49 (8) | 5.28 (15) | 1.81 (8) | 0.000 (0) | 0.04 (7) | 0.000 (0) |
| H6 | N | 1.73 (7) | 5.15 (15) | 2.59 (9) | 0.000 (0) | −0.03 (7) | 0.000 (0) |
| H5 | N | 1.46 (7) | 5.72 (17) | 3.77 (11) | 0.000 (0) | 1.10 (7) | 0.000 (0) |
| H21 | N | 4.78 (20) | 3.32 (17) | 3.78 (15) | −1.13 (15) | 2.73 (15) | −1.37 (14) |
| H22 | N | 2.19 (10) | 6.94 (32) | 1.87 (9) | 0.01 (12) | 0.43 (8) | 0.82 (11) |
| H31 | N | 3.72 (15) | 5.61 (21) | 2.45 (12) | −0.36 (16) | 1.96 (11) | −0.07 (14) |
| H32 | N | 3.67 (14) | 2.37 (13) | 3.95 (15) | −0.04 (11) | 1.78 (13) | 0.50 (11) |
| H41 | N | 4.50 (26) | 3.66 (18) | 4.14 (17) | 1.40 (18) | 2.61 (19) | −0.03 (15) |
| H42 | N | 2.52 (16) | 6.35 (30) | 4.01 (17) | −1.27 (19) | 1.88 (14) | 0.30 (19) |

[a] N: Refinement based on neutron data at 0.894 Å. X: X-ray all-data refinement. XH: X-ray high-order refinement.

tribution in this donor–acceptor bond has to be compared with that in other pyridine derivatives. The density determinations

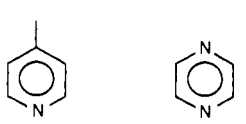

2



3

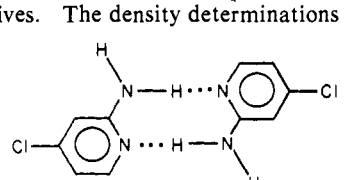

4

of 4-picoline[23] (**2**) and pyrazine[24] (**3**) display examples where the tertiary nitrogen does not form interatomic connections significantly shorter than van der Waals interactions. In 4-picoline the center of the lone-pair density (0.4 e/Å$^3$) is in the plane through the ring atoms outside the cycle in the bisecting position (C–N–C) about 0.6 Å from N. This distance is comparable with the 0.7

(23) Heger, G.; Ohms, U.; Treutmann, W. *Acta Crystallogr., Sect. A* **1981**, *A37S*, 208. Ohms, U.; Guth, H.; Treutmann, W.; Heger, G. *Rep. Kernforschungszentrum Karlsruhe* **1981**, *No. KfK 3381*, 38.

(24) De With, G.; Harkema, S.; Feil, D. *Acta Crystallogr., Sect B* **1976**, *B32*, 3178.

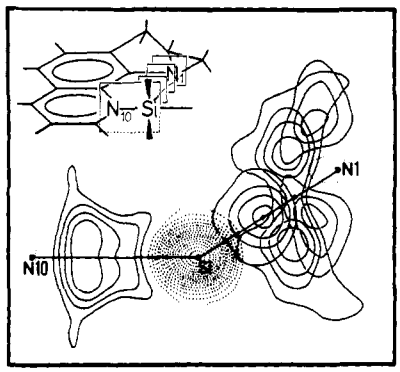


**Figure 7.** Deformation density in the two different Si–N bonds. Left: section through the Si–N10 bond. Right: parallel sections perpendicular to the Si–N1 bond (contours as in Figure 3).

Å of the present study. From the center the density of this peak decreased symmetrically to both sides along the direction which aligns the ring bisector through nitrogen and the methyl group. No perturbation of the lone-pair density on nitrogen due to a polarizing neighbor as detected in the donor–acceptor bond of **1** is observed in 4-picoline and pyrazine.

The density distribution in the lone-pair region at the pyridine nitrogen of 2-amino-5-chloropyridine (**4**),[25] however, exhibits a distortion due to an intramolecular hydrogen bond (N···H) = 2.051 Å). The center of the lone pair on the pyridine nitrogen (0.5 e/Å$^3$) points in the direction of the hydrogen atom and is slightly polarized along the bond axis toward H. The density gradient is therefore smaller on the side toward hydrogen than the one close to the pyridine nitrogen. These observations are in qualitative agreement with our results on **1**.

**The Si–N1 Bond.** The Si–N1 bond (1.746 (2) Å) is 6.6% shorter than the sum of covalent radii for Si and N. In many studies partial "double bonding character" of the Si–N connection was postulated to explain this "bond shortening". To properly discuss the density distribution in this bond, some review of bond lengths in coordination compounds of Si–N and Si–C derivatives is mandatory. Similar covalent radii of carbon and nitrogen may be assumed as rough approximation. Brook et al.[26] determined the Si–C distance in a crystalline silaethylene to 1.764 (3) Å. In this compound Si and C are both connected to three nearest neighbors. They are described by a "sp$^2$-hydridization", and a "double bonding character" is attributed to the central Si–C bond. The molecule is twisted by 14.6° about this Si–C bond which may be due to the bulkiness of the substituents or to packing forces in the crystalline state. Brook and co-workers assume that there are no reasons to invoke significant stretching of the bond due to steric effects. Several molecular orbital calculations for simple silaethylenes yielded shorter Si–C bonds. In comparison, Si–C bonds in silicon compounds with tetravalent C display values between 1.86 and 1.91 Å. A distance of 1.75 Å results as arithmetic mean of the Si–N distance between a tetra- or pentavalent silicon and a trivalent nitrogen.

Recently we determined the Si–N bond length in the ionic silicon compounds (py)$SiMe_3^+X^-$ (X = Br, I) where Si and N might be described as tetravalent.[27] In both structures the bond length is 1.86 Å. This value matches the Si–C distances in most tetravalent Si–C compounds and is close to the value predicted from the sum of covalent radii.

Two interesting conclusions may be drawn from this simple comparison. The Si–N distance in **1** and in many Si–N derivatives aligns with the Si–C distance in the silaethylene which was described as a Si–C "double bond". Next, the "shortened" distance

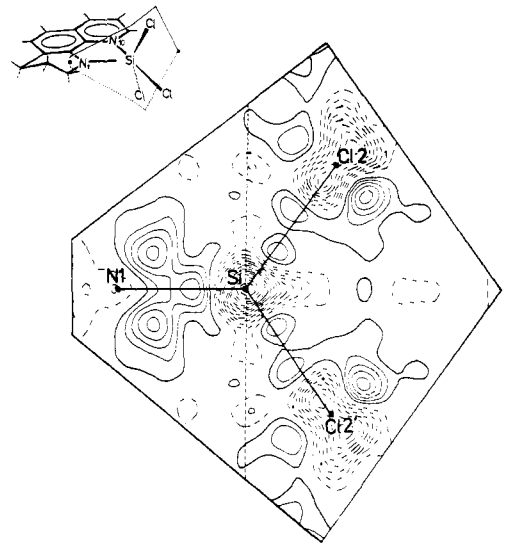


**Figure 8.** Deformation density in the trigonal base plane through N1, Si, Cl2, Cl2′ (contours as in Figure 3); this plane is slightly faulted along the dashed line.

of about 1.75 Å is only observed if C and N are trivalent (silaethylene, silazanes with trivalent N). In compounds with tetravalent carbon or nitrogen ("normal" Si–C derivatives and (py)$SiMe_3^+X^-$, where three valences of nitrogen are "used" to interact in the aromatic cycle) a bond length of about 1.86 Å is found.

In the light of these results, the deformation density in the short Si–N1 bond of the title compound can be discussed. The map through the molecular plane (Figure 4) reveals a maximum of 0.4 e/Å$^3$ between Si and N1. It is more concentrated along the bond axis than the density in the donor–acceptor bond.

Of greater interest is the density distribution perpendicular to the molecular plane through this bond. Solely based on geometrical parameters the electronic state at nitrogen might be associated with a "sp$^2$-hydridization". In agreement with the stereochemical predictions of the sp$^2$-hydridization model the three direct neighbors on N1 are in a planar arrangement. This result would suggest that the lone-pair density at N1 is located perpendicular to the molecular plane above and below the position of N1. On the right-hand side of Figure 6, a section through Si and N1 orthogonal to the molecular plane is shown. As expected, two density maxima are found above and below the site of N1. But their centers are significantly displaced in direction to silicon. In Figure 7 (right-hand side) a series of staggered sections perpendicular to the bond axis and the molecular plane elucidates the density distribution around the Si–N1 bond. As an explanation for this displacement we suggest a polarization of the lone-pair density at N1 by silicon. With some care this release of electron density from the position upon N1 into the Si–N1 bond might be considered to explain the apparent discrepancy between the observed bond lengths in silazanes and the predictions based on the sum of covalent radii.

**The Si–Cl Bonds.** Three sites on the trigonal bipyramid around silicon are occupied by chlorine. As a consequence two topologically different Si–Cl bonds are present. Both are extended as compared with Si–Cl distances (~2.04 Å) in tetravalent chlorosilanes. Sections through these bonds are presented in Figures 4, 5, and 8. In agreement with other studies, the density in the Si–Cl bonds is rather low.[25,28] The chlorine atoms are surrounded by residual density which might be interpreted as lone-pair density around these atoms. It is known from nucleophilic substitution that Cl is a rather good leaving group (displaced as $Cl^-$). The arrangement in **1** shares similarities with an intermediate state of the $S_N2$ reaction pathway.[1] It seems reasonable that the chlorine atoms are negatively polarized and slightly charged in connections to silicon which are fairly extended.

(25) Kvick, A.; Thomas, R.; Koetzle, T. F. *Acta Crystallogr., Sect. B* **1976**, *B32*, 224.
(26) Brook, A. G.; Nyburg, S. C.; Abdesaken, F.; Gutekunst, B.; Gutekunst, G; Kallury, R. K. M. R. Poon, Y. C.; Chang, Y. M.; Ng, W. W. *J. Am. Chem. Soc.* **1982**, *104*, 6557.
(27) Hensen, K.; Zengerly, T.; Pickel, P.; Klebe, G. *Angew. Chem.* **1983**, *98*, 973; *Angew. Chem. Int. Ed. Engl.* **1983**, *22*, 725.
(28) Cohen-Addad, C.; Savariault, J. M.; Lehmann, M. S. *Acta Crystallogr., Sect. B.* **1981**, *B37*, 1703.

Nevertheless, density around Cl has to be interpreted with great care, because accuracy in density distribution near the atomic positions, especially of heavier atoms, decreases rapidly due to the uncertainty in scale factor and experimental errors in positional and thermal parameters.

## Conclusion

As noted in the introduction, **1** and closely related chelated complexes exhibit dynamic behavior in solution, which results from the lability of coordinative bonding. Positional exchange of substituents at pentacoordinate Si is performed throughout a low-energy barrier by fission and re-formation of the coordinative bond together with the rotation of the intermediate four-coordinate silyl substituent around the "single bond" connection between the ligand skeleton and the silyl group (Scheme I).

The present density study shows that two effects have to be considered when the influence of bonding to silicon on the rotation barrier is discussed. It reveals the donor–acceptor bond as a lone pair on the pyridine-type nitrogen which is heavily polarized by silicon. An influence of this interaction on the barrier to rotation in solution seems likely. Furthermore, it shows that the lone pair on the amino-type nitrogen N1 of the higher saturated heterocycle is shifted into the Si–N bond. This anisotropic charge distribution between Si and N1 may possibly increase the rotation barrier, because N1 acts as a pivot during the rotation of the silyl group in the rearrangement in solution. This conclusion is supported by temperature-dependent NMR studies of the above-mentioned silaethylenes[26] which show in solution up to 60 °C no evidence of rotation about the central Si–C bond which is assumed to possess "multiple bonding character". This fact might be seen as an indication that this bond is kinetically stable against internal rotations, but any conclusions on the height of the barrier quoted as activation enthalpy can only be derived if dynamic NMR properties are observed and evaluated as a function of temperature.

**Acknowledgment.** We thank J. M. Savariault, M. S. Lehmann, and J. R. Allibon (ILL, Grenoble) for technical assistance with the neutron diffraction experiment. We gratefully acknowledge the help of the Institut für Kernphysik (Universität Frankfurt) for making the diffractometer available. This work has been supported by the Bundesministerium für Forschung und Technologie and by the Deutsche Forschungsgemeinschaft.

**Registry No. 1**, 78271-96-2.

**Supplementary Material Available:** Listing of the observed and calculated structure factors of the three data sets (neutrons, 0.894 Å, 1.266 Å, X-rays, 0.71069 Å) (34 pages). Ordering information is given on any current masthead page.

# Highly Enantioselective Isomerization of Prochiral Allylamines Catalyzed by Chiral Diphosphine Rhodium(I) Complexes. Preparation of Optically Active Enamines[1]

**Kazuhide Tani,*[2a] Tsuneaki Yamagata,[2a] Susumu Akutagawa,[2b] Hidenori Kumobayashi,[2b] Takanao Taketomi,[2b] Hidemasa Takaya,[2c] Akira Miyashita,[2c] Ryoji Noyori,[2d] and Sei Otsuka*[2a]**

*Contribution from the Department of Chemistry, Faculty of Engineering Science, Osaka University, Toyonaka, Osaka, Japan 560, Central Research Laboratory, Takasago Perfumery Co. Ltd., 31-36, 5-chome, Kamata, Ohta-ku, Tokyo, Japan 144, Chemical Materials Center, Institute for Molecular Science, Okazaki, Japan 444, and Department of Chemistry, Faculty of Science, Nagoya University, Chikusa, Nagoya, Japan 464.* *Received December 19, 1983*

**Abstract:** Rh(I) complexes of types $[Rh(diphosphine)(diene)]ClO_4$ and $[Rh(diphosphine)(S)_n]ClO_4$ (diphosphine = cis-chelating tertiary diphosphine; diene = 1,5-cyclooctadiene or norbornadiene; S = solvent) were found to be effective catalysts for allylic hydrogen migration of tertiary and secondary allylamines to give the corresponding (*E*)-enamines and imines, respectively. Studies on diphosphine ligands with respect to the catalytic activity and product selectivity led to the discovery of a fully aryl-substituted diphosphine, BINAP [2,2′-bis(diphenylphosphino)-1,1′-binaphthyl], which produces very active Rh(I) complex catalysts. With $[Rh((\pm)\text{-BINAP})(COD)]ClO_4$ (COD = 1,5-cyclooctadiene) or $[Rh((\pm)\text{-BINAP})(S)_n]ClO_4$ as catalyst, (*Z*)-(diethylnerylamine, **1**) or (*E*)-*N*,*N*-diethyl-3,7-dimethyl-2,6-octadienylamine (diethylgeranylamine, **2**) was isomerized into the racemic (*E*)-enamine (*E*)-*N*,*N*-diethyl-3,7-dimethyl-1,6-octadienylamine (citronellenamine, **3**) with a chemical selectivity of over 95%, the 6-double bond being retained intact. A variety of substituted allylamines serves as the substrate, e.g., (*E*)-*N*,*N*-dimethyl-2-butenylamine, *N*,*N*-dimethyl-2-methyl-2-propenylamine, *N*,*N*-dimethyl-3-methyl-2-butenylamine, *N*,*N*-dimethyl-3-phenyl-2-butenylamine. Asymmetric isomerization of prochiral allylamines producing optically active enamines or imines can be effected with cationic Rh(I) complexes of various chiral diphosphine ligands such as (2*R*,3*R*)-DIOP and others. The ligand that gives the highest optical yield was (+)- or (−)-BINAP. Virtually perfect enantioselectivity (95–99% ee) was achieved with $[Rh((+)\text{- or } (-)\text{-BINAP})(COD)]^+$ for the isomerization of **1** or **2** into the optically active (*E*)-enamine (**3**). A clear stereochemical correlation was established between the olefin geometry (*E* or *Z*) of substrates, the configuration of the chiral diphosphines (*R* or *S*), and the chiral carbon configuration of the product enamines (*R* or *S*). The present catalytic system thus provides a convenient and practical access to optically active aldehydes. For example, optically pure natural citronellal can be produced either from nerylamine with the Rh(I)–(+)-BINAP catalyst or from geranylamine with the Rh(I)–(−)-BINAP complex catalyst.

Olefin double-bond migration is one of the most extensively studied catalytic reactions. The isomerization is involved frequently in such transition-metal catalysis as hydroformylation, oligomerizations, and other reactions.[3,4] Although the catalysis

(1) Metal-Assisted Terpenoid Synthesis. 7. For part 6, see: ref 27.
(2) (a) Osaka University. (b) Takasago Perfumery Co. Ltd.. (c) Institute for Molecular Science. (d) Nagoya University.

(3) For some reviews, see: (a) Parshall, G. W. "Homogeneous Catalysis"; Wiley: New York, 1980; Chapter 33. (b) Rylander, P. N. "Organic Syntheses with Noble Metal Catalysts"; Academic Press: New York, 1973; Chapter 5.

0002-7863/84/1506-5208$01.50/0 